ACS Sustainable Chemistry & Engineering

pubs.acs.org/journal/ascecg

Research Article

Enabling $LiNi_{0.88}Co_{0.09}Al_{0.03}O_2$ Cathode Materials with Stable Interface by Modifying Electrolyte with Trimethyl Borate

Zhen-Xue Xiao,[†] Shao-Lun Cui,[†] Yang-Yang Wang, Sheng Liu, Guo-Ran Li,* and Xue-Ping Gao

Cite This: *ACS Sustainable Chem. Eng.* 2021, 9, 1958−1968

Read Online

ACCESS | Metrics & More | Article Recommendations | Supporting Information

ABSTRACT: As one of the most promising cathode materials in lithium-ion batteries, nickel-rich cathode materials have been widely studied due to their high specific capacity and high operating voltage to realize the energy density of 300 Wh kg^{-1}. However, the oxidative decomposition of electrolyte catalyzed by transition metal ions and the crack of secondary particles have brought great challenges to their further development. In order to solve this problem, functionalized electrolyte is often used to stabilize the interface and structure of cathode materials. Herein, it is proposed to add trimethyl borate (TMB) in commercial electrolyte to enhance the interfacial stability of Li-$Ni_{0.88}Co_{0.09}Al_{0.03}O_2$ cathode material. By adjusting the content of TMB in the electrolyte, it is found that a volume ratio of 10% can achieve the best electrochemical performance. In the voltage range of 3.0−4.3 V, the $LiNi_{0.88}Co_{0.09}Al_{0.03}O_2$ electrode with the 10% TMB-containing electrolyte can achieve a capacity retention of up to 82% after 300 cycles at 1C rate (1C = 200 mA g^{-1}), while the electrode with blank electrolyte is only 61%. Through a systematic analysis toward cycled electrode materials, it is indicated that the cracking degree of secondary particles decreases and a thin, stable, and conductive cathode electrolyte interface film is formed on the electrode with 10% TMB-containing electrolyte. This simple and effective method of improving the interfacial and structural stability of nickel-rich cathode materials via adding TMB in the electrolyte provides a practical strategy for the development of high-performance lithium-ion batteries.

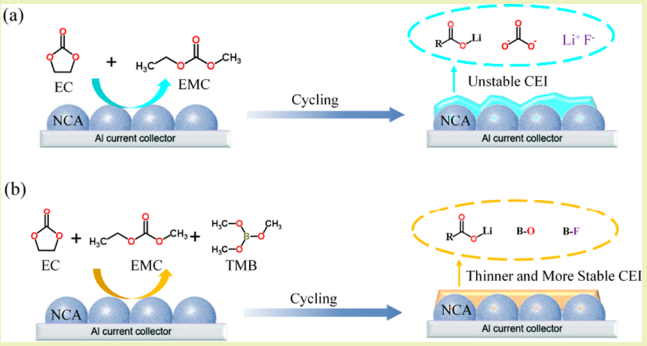

KEYWORDS: *Ni-rich cathode material, Stable interface, Trimethyl borate, Electrolyte additive, Li-ion battery*

INTRODUCTION

With the increasing demands for portable electronic devices, electric vehicles, and large-scale energy storage equipment, lithium-ion batteries have developed rapidly in the past three decades as the main power source.[1] And the overall energy density in the battery system mainly depends on the electrochemical properties of cathode materials.[2] Currently, layered $LiCoO_2$, ternary $LiNi_xCo_yMn_{1-x-y}O_2$ (NCM), spinel $LiMn_2O_4$, and olivine $LiFePO_4$ are the most commonly used cathode materials in lithium-ion batteries. Among them, nickel-rich layered oxides, including $LiNi_xCo_yMn_{1-x-y}O_2$ ($x \geq 0.6$) and $LiNi_xCo_yAl_{1-x-y}O_2$ ($x \geq 0.6$), are the most promising cathode materials to attain the energy density of 300 Wh kg^{-1}. Simultaneously, their advantages such as higher specific capacity, higher midpoint voltage, and lower cost have attracted wide attention of researchers. However, there are still many unsolved severe challenges facing the future development of Ni-rich cathode materials. During the charge-discharge process, ester-based electrolytes are more likely to be oxidized and decomposed into CO and CO_2 gases under the catalysis of transition metal ions.[2] At the same time, the secondary particles of cathode materials will generate pores or even cracks due to the increase of internal stress, especially at high charging potentials, resulting in poor electrochemical performance of the battery.[3] Therefore, a lot of effective modification strategies such as surface coating, bulk doping, and structural design are applied to improve the structural and interfacial stability of the electrode.

Surface coating is a widely used method to protect active materials from erosion of electrolyte by reducing parasitic side reactions on the interfaces. At the same time, unfavorable phase transformation and bulk crack can be effectively suppressed. At present, oxides (Al_2O_3,[4,5] MgO,[6,7] Y_2O_3[8]), phosphates (H_3PO_4,[9] $AlPO_4$,[10,11] $SnPO_4$,[12] $NiPO_4$,[13] $CoPO_4$,[14] $FePO_4$[15]), fluorides (CaF_2,[16] CeF_3,[17] AlF_3,[17] $LiTiF_2$[18]), carbons,[19−21] conducting polymers,[22,23] Li^+-conductor ($LiFePO_4$,[24] $LiMnPO_4$,[25] $NaTi_2(PO_4)_3$,[26] Li_3PO_4,[27,28]

Received: December 22, 2020
Revised: January 6, 2021
Published: January 20, 2021

https://dx.doi.org/10.1021/acssuschemeng.0c09241
ACS Sustainable Chem. Eng. 2021, 9, 1958−1968

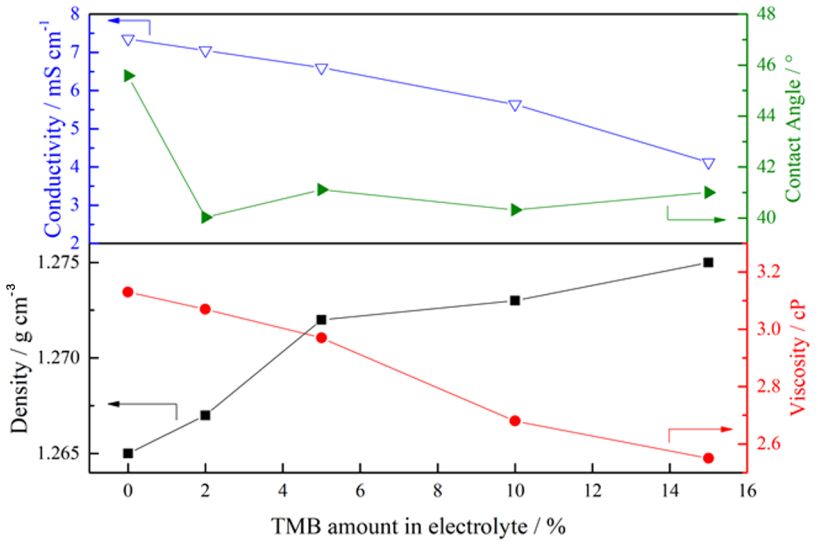

Figure 1. Conductivity, contact angle, density, and viscosity results of blank electrolyte and electrolytes with TMB.

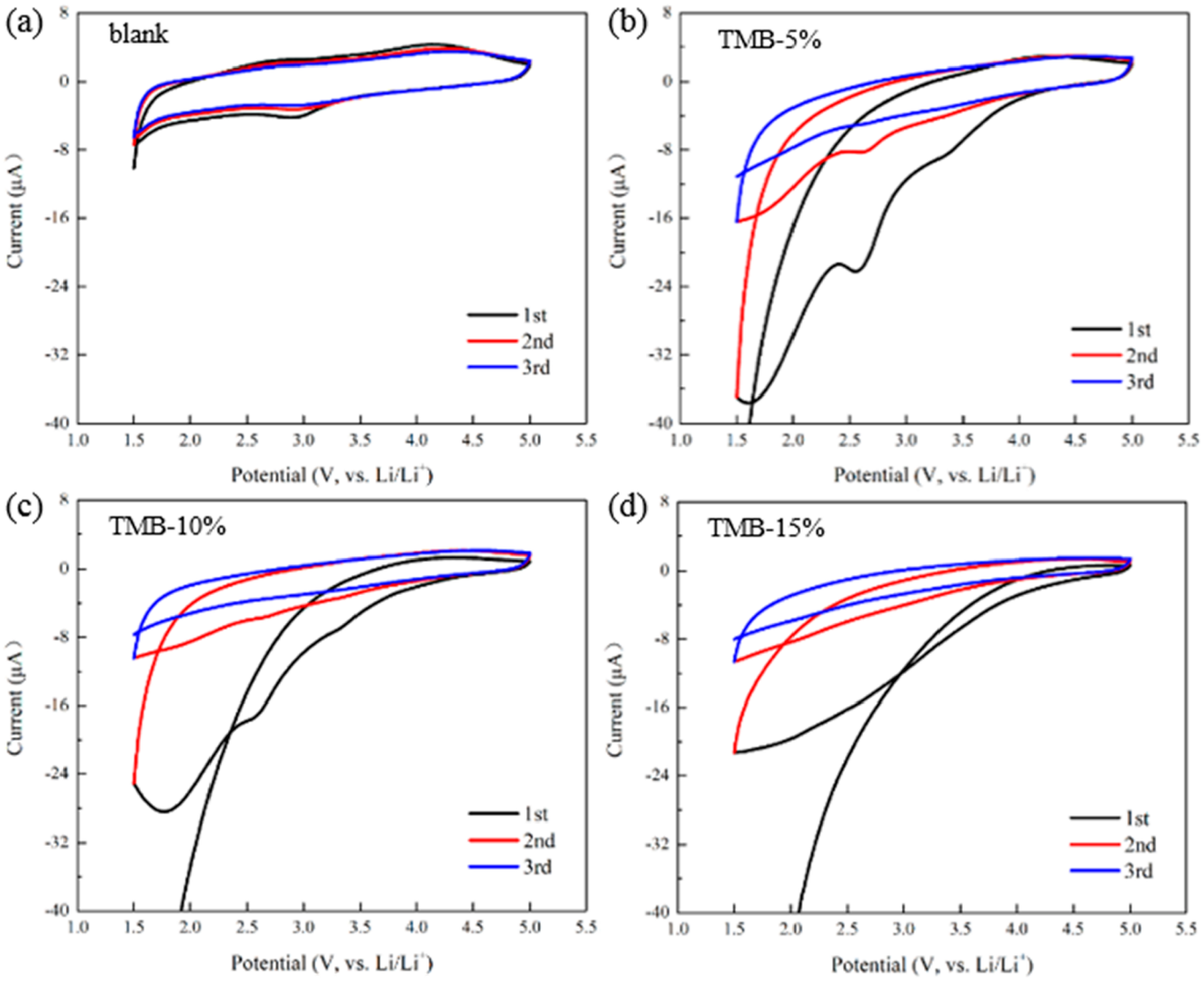

Figure 2. Cyclic voltammograms (CV) of (a) blank, (b) 5%, (c) 10%, and (d) 15% TMB-containing electrolytes at a scan rate of 0.5 mV s^{-1}.

Li_2O-BPO_4[29]), and core−shell structure[30] have been used for surface modification. Nevertheless, it is not easy to form a uniform and compatible coating layer on the surface of electrode particles.[31−33] Instead, forming a firm interfacial film

https://dx.doi.org/10.1021/acssuschemeng.0c09241
ACS Sustainable Chem. Eng. 2021, 9, 1958−1968

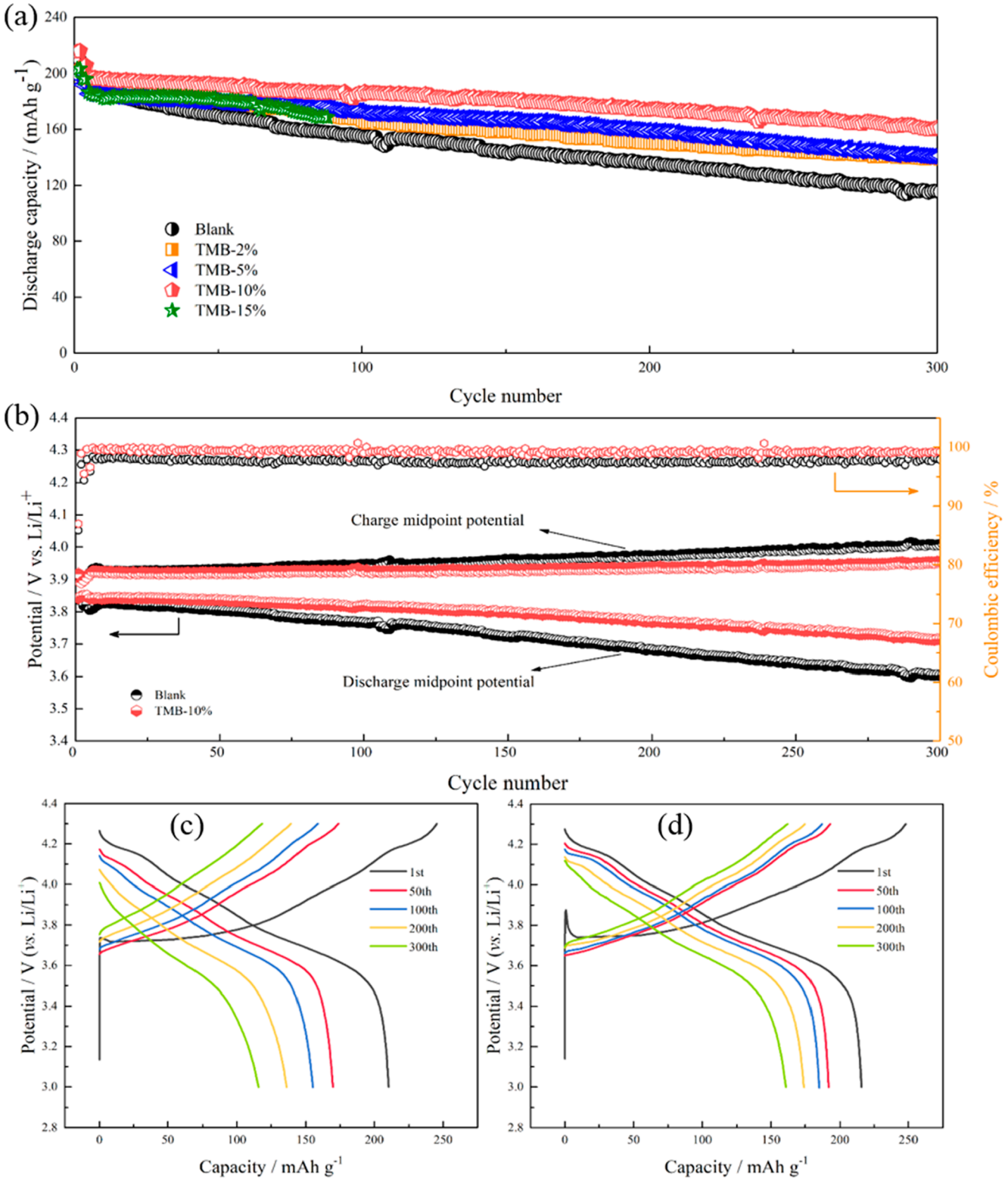

Figure 3. (a) Cycle performance of $LiNi_{0.88}Co_{0.09}Al_{0.03}O_2$ with different contents of TMB in the voltage range of 3.0−4.3 V at 30 °C. (b) Midpoint voltage curves of $LiNi_{0.88}Co_{0.09}Al_{0.03}O_2$ with blank and 10% TMB-containing electrolytes. (c, d) Charge/discharge curves of $LiNi_{0.88}Co_{0.09}Al_{0.03}O_2$ at selected cycles in blank and 10% TMB-containing electrolytes (1C rate).

at the interface by adding a functional chemical substance into the electrolyte is a simple and economical way to improve the structural and electrochemical stability of cathode materials.[34−36] Electrolyte additives are reported to be able to suppress the decomposition of electrolyte solvents, thereby forming a protective film on the particles to avoid electrolyte corrosion and crystal breakdown.[37] Since boron is an electron-deficient element, boron-containing compounds are prone to

https://dx.doi.org/10.1021/acssuschemeng.0c09241
ACS Sustainable Chem. Eng. 2021, 9, 1958−1968

form complexes with anions, such as F^- and PF_6^-. Boron in the additives is also considered to be involved in the formation of the cathode electrolyte interface (CEI) film, which means that boron element coordinates with F^- to dissolve LiF out of the CEI film and promotes the formation of a more stable CEI film.[38] Previously, trimethyl borate (TMB) has been investigated as a film-forming additive that can significantly improve the performance of lithium-ion cathode materials. For example, Liu et al.[39] reported that $LiCoO_2$ could deliver a capacity retention of 81% with 2.0 wt % TMB-containing electrolyte, but only 64% in the blank electrolyte. Chang et al.[40] demonstrated the electrochemical performance of $LiFePO_4$ with 0.1 M TMB in the electrolyte was greatly improved after 100 cycles and the thermal decomposition was suppressed at 60 °C. Additionally, TMB is also applied in Ni-based cathode materials and significantly promotes the cycle performance of $LiNi_{1/3}Co_{1/3}Mn_{1/3}O_2$.[41] Therefore, it is worth considering what effects TMB as an electrolyte additive can bring for nickel-rich cathode materials.

In this study, different contents of TMB are used as an electrolyte additive to improve the electrochemical performance of $LiNi_{0.88}Co_{0.09}Al_{0.03}O_2$. And the blank electrolyte composition is 1 M $LiPF_6$ in EC/EMC (3/7, v/v). Through the characterization of a series of electrochemical properties and structural characteristics, it is found that the electrode using 10% TMB-containing electrolyte displays the best performance. Compared with the blank electrolyte, the capacity retention of $LiNi_{0.88}Co_{0.09}Al_{0.03}O_2$ with TMB increases from 61% to 82% after 300 cycles at 1C rate. According to the detailed information from scanning electron microscopy (SEM), X-ray photoelectron spectroscopy (XPS), transmission electron microscopy (TEM), and Fourier transform infrared spectroscopy (FTIR), it is easy to observe that a more stable and conductive CEI film is formed on the surface of the cathode material. It can not only prevent the decomposition of the electrolyte but also suppress the structure degradation of the bulk phase. As a result, the cycle and rate performance of $LiNi_{0.88}Co_{0.09}Al_{0.03}O_2$ are remarkably improved by adding TMB into the electrolyte. This simple and practical method can greatly benefit industrial production and further promote the commercialization process of nickel-rich cathode materials.

RESULTS AND DISCUSSION

The conductivity, contact angle, density, and viscosity results of blank electrolyte and electrolytes with different contents of TMB are shown in Figure 1. It is clear to see that the conductivity, contact angle, and viscosity of the electrolyte decrease roughly with the increase of the content of TMB in the electrolyte, while the density of the electrolyte presents the opposite trend. Generally, the decrease of contact angle and viscosity is favorable for improving the whole electrochemical performance of the battery. On one hand, it can ensure sufficient penetration at the interface between nickel-rich cathode materials and electrolyte. On the other hand, it can improve the fluidity of the electrolyte. Therefore, it can be affirmed that the addition of TMB facilitates the diffusion and transport of lithium ions. Conductivity is one of the most important parameters that evaluate the property of an electrolyte. As the content of TMB in the electrolyte increases, its conductivity tends to decrease slowly. This indicates that the TMB content needs to be controlled at a certain level; otherwise, it may affect its conductivity. Although the density of the electrolyte increases slightly after adding TMB, it remains basically unchanged. The detailed data of conductivity, contact angle, density, and viscosity for an electrolyte are shown in Table S1 and Figure S1 (Supporting Information).

To confirm the electrochemical stability of electrolytes involving TMB, the cyclic voltammetry (CV) tests with a wide voltage range from 1.5 to 5.0 V are performed. It is found from Figure 2 that, at the very beginning, there are relatively large currents in the region of low voltages, implying reduction of TMB. Moreover, the initial currents rise with increasing content of TMB additive. From the second cycle, the currents are very close in the cases with different amounts of TMB. This reveals that reduction of TMB mainly occurs in the first cycle especially in the range of low voltage. After the first cycle, the electrolyte with TMB generally can be kept stable in the sequential cycles. More importantly, the electrolytes with TMB are electrochemically stable in the voltage range of 3.0−4.3 V that usually is used for NCA cathode materials. It means that TMB can be practically used as an electrolyte additive for NCA cathode materials and seldom brings about adverse effects to the electrolyte.

The cycle performance of $LiNi_{0.88}Co_{0.09}Al_{0.03}O_2$ at 30 °C in the blank, 2%, 5%, 10%, and 15% TMB-containing electrolytes is displayed in Figure 3a. It is clear to observe that the cycle stability of the cathode material with TMB additive is obviously better than that using the blank electrolyte. And the $LiNi_{0.88}Co_{0.09}Al_{0.03}O_2$ cathode material in the 10% TMB-containing electrolyte shows the most superior electrochemical performance. It delivers an initial capacity of 196.6 mAh g^{-1} with a capacity retention of 81.79% after 300 cycles at 1C rate, which is significantly higher than that of 189.7 mAh g^{-1} and 60.83% in the blank electrolyte. The serious capacity decay of the $LiNi_{0.88}Co_{0.09}Al_{0.03}O_2$ material in the blank electrolyte originates from the decomposition of electrolyte and the crystal destruction of secondary particles.[42] On the contrary, when TMB is added into the blank electrolyte, a protective film is formed on the surface of the $LiNi_{0.88}Co_{0.09}Al_{0.03}O_2$ material, which can inhibit further decomposition of the electrolyte and protect the electrode from crystal cracking.[43]

Figure 3b shows the evolution of Coulombic efficiency and midpoint voltage of nickel-rich cathode materials. Apparently, the Coulombic efficiency of the battery with 10% TMB-containing electrolyte is close to 100%, which is also higher than that of the blank electrolyte. At the same time, the addition of 10% TMB in the electrolyte can obviously suppress the midpoint voltage decay and decrease the potential gap of the battery compared with the blank electrolyte. Figure 3c,d shows the charge/discharge curves of $LiNi_{0.88}Co_{0.09}Al_{0.03}O_2$ materials in the blank electrolyte and 10% TMB-containing electrolyte during long cycling. The cathode material with blank electrolyte shows a rapid capacity fade and continuous increase of overpotential during cycling, which results from the formation of a thick and resistive CEI film on the surface of electrodes. By contrast, the CEI film formed in 10% TMB-containing electrolyte is thinner and easier to transport of Li^+ ions.[44]

The rate capability of $LiNi_{0.88}Co_{0.09}Al_{0.03}O_2$ with blank electrolyte and 10% TMB-containing electrolyte is shown in Figure 4. It is found that the rate performance of cells with TMB is much better than that with the blank electrolyte, especially at high rates. This is because the overall resistances of the electrode with TMB-contianing electrolyte are lower than that with blank electrolyte after activation of electrodes at the low rate, which is beneficial for diffusion of Li^+ and

https://dx.doi.org/10.1021/acssuschemeng.0c09241
ACS Sustainable Chem. Eng. 2021, 9, 1958−1968

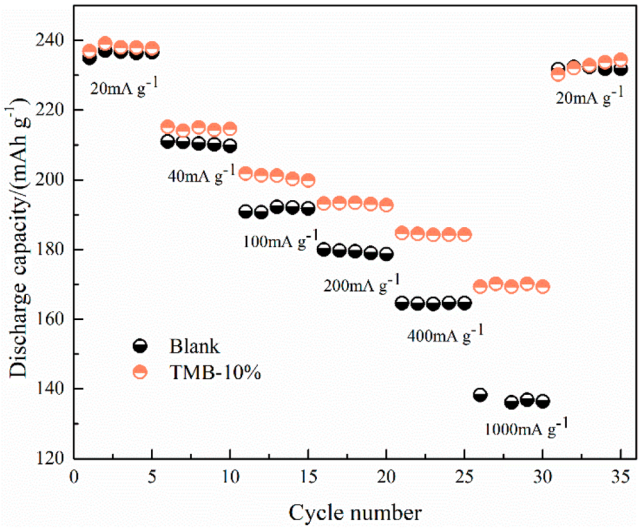

Figure 4. Rate performance of $LiNi_{0.88}Co_{0.09}Al_{0.03}O_2$ in blank and 10% TMB-containing electrolytes (1C = 200 mA g^{-1}).

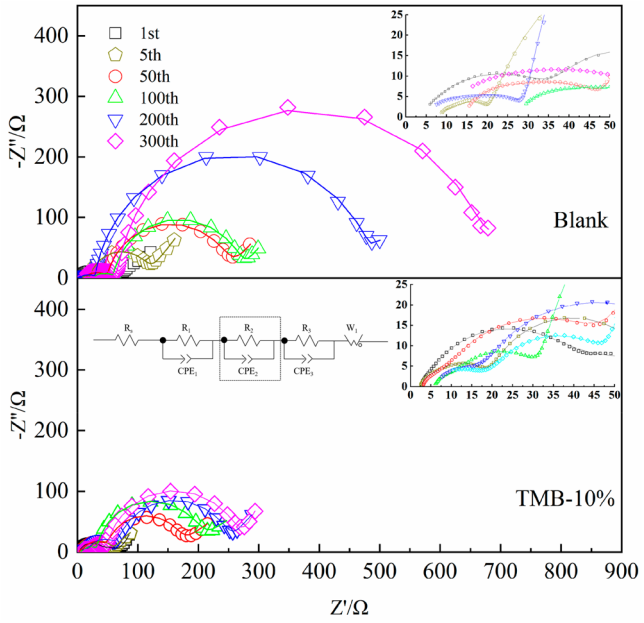

Figure 5. Electrochemical impedance spectra of $LiNi_{0.88}Co_{0.09}Al_{0.03}O_2$ in blank and 10% TMB-containing electrolytes.

delivering a high discharge capacity. Especially, when the rate is 5C (1000 mA g^{-1}), cathode materials with 10% TMB-containing electrolyte maintain a discharge capacity of about 170 mAh g^{-1}, which is much higher than that of about 140 mAh g^{-1} with blank electrolyte. It is noteworthy that, even if the charge cutoff voltage has increased, TMB still can work. As the charge cutoff voltage rises from 4.4 to 4.7 V, the cathode material with TMB can significantly suppress the capacity decay compared to that with blank electrolyte (Figure S2, Supporting Information). It has proved that TMB additive is still beneficial for the cycle performance of $LiNi_{0.88}Co_{0.09}Al_{0.03}O_2$ materials even at a higher cutoff voltage.

The dQ/dV curves of $LiNi_{0.88}Co_{0.09}Al_{0.03}O_2$ with blank and 10% TMB-containing electrolytes at different cycles are presented in Figure S3 (Supporting Information). There are three pairs of peaks on both profiles which correspond to three kinds of phase transitions for nickel-rich cathode materials. In the blank electrolyte, the peak position of $LiNi_{0.88}Co_{0.09}Al_{0.03}O_2$ changes constantly and the peak intensity gradually weakens. However, the peak position and peak intensity for $LiNi_{0.88}Co_{0.09}Al_{0.03}O_2$ with 10% TMB-containing electrolyte gain relatively small changes. The addition of TMB in the electrolyte can suppress the harmful phase transition of nickel-rich cathode materials.

Electrochemical impedance spectra (EIS) are conducted to study the effect of TMB additive on electrochemical properties of electrodes. Figure 5 presents the Nyquist plot of electrodes with blank and 10% TMB-containing electrolytes, the enlarged spectra at high frequency, and the equivalent circuit. Except for the first cycle, the other Nyquist plots are composed of three semicircles and an inclined line, which attributes to the surface film resistance (R_1), charge transfer resistance (R_2), Nernst diffusion resistance[45] (R_3), and Warburg resistance, respectively.[46] R_1 reflects the resistance of the CEI film, R_2 represents the charge-transfer resistance for lithiation/delithiation, R_3 shows the finite diffusion of Li^+ in the CEI film, and W_f is attributed to the Li^+ diffusion impedance in the electrode. It is well-known that the formation of CEI film is a complex process involving the decomposition of electrolyte and interfacial side reaction at the activation stage of electrodes. And the TMB participates in the formation of the CEI film. As a result, the surface film resistance is larger in the first cycle and the surface film resistance of the electrode with 10% TMB-containing electrolyte is higher than that with blank electrolyte at the initial stage. After activation of electrodes, the surface film resistance increases with cycling of the electrode, which means the electrolyte is constantly decomposed and involved in the formation of the CEI film. However, the resistance values of the electrode with blank electrolyte are larger than those with the 10% TMB-containing electrolyte except for the 200th cycle. It is assumed that the particles are cracked and the fresh surface is exposed in the electrolyte after around 200 cycles. As a result, the surface film resistance decrease correspondingly. As the cracks intensify, the CEI film becomes thicker and thicker, leading to a leap in surface film resistance. Oppositely, the surface film resistance of the electrode with 10% TMB-containing electrolyte increases steadily and slowly, which means the stable and protective CEI film is generated. And the Nernst diffusion resistance of the electrode with blank electrolyte is significantly higher than that of the electrolyte containing 10% TMB. It means that the Li^+ is easier to diffuse in the CEI film of the electrode with 10% TMB-containing electrolyte. More detailed EIS data and the Bode plots are shown in Table S2 and Figure S4 (Supporting Information). In general, with cycling of the electrode, the electrolyte is constantly decomposed and the CEI film is continually growing. As a result, the surface film resistance and Nernst diffusion resistance increase. However, the CEI film generated in the TMB-containing electrolyte is more stable and protective, which inhibits the rapid increase of resistance. In addition, as an electron-deficient compound, TMB can cooperate with F^- to enhance the solubility of LiF in the CEI film, thereby increasing its ionic conductivity.[47]

Figure 6 presents the SEM images of the $LiNi_{0.88}Co_{0.09}Al_{0.03}O_2$ materials before and after 300 cycles. It can be clearly observed that the nickel-rich cathode material is composed of spherical secondary particles with a diameter of about 10−15 μm, as shown in Figure 6a,b. After 300 cycles, a number of secondary particles of the cycled cathode materials

https://dx.doi.org/10.1021/acssuschemeng.0c09241
ACS Sustainable Chem. Eng. 2021, 9, 1958−1968

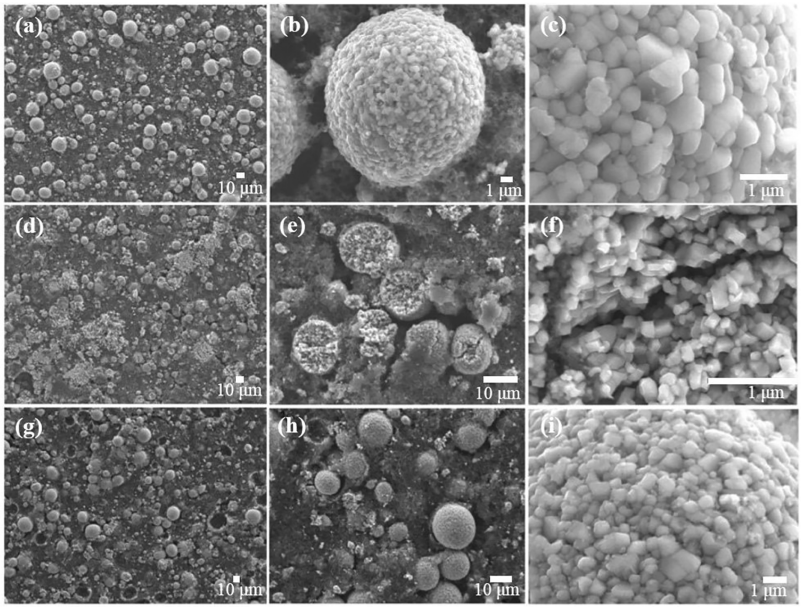

Figure 6. SEM images of $LiNi_{0.88}Co_{0.09}Al_{0.03}O_2$ materials before cycling (a–c) and after 300 cycles in blank electrolyte (d–f) and 10% TMB-containing electrolyte (g–i).

in the blank electrolyte are pulverized (Figure 6d,e). By contrast, there are almost no secondary particles cracked in the 10% TMB-containing electrolyte, which is close to the fresh state in Figure 6g,h. The cracked particles in the blank electrolyte are further compared with the complete particles in the 10% TMB-containing electrolyte, and it is found that the surface of the cracked particles looks relatively loose and has large cracks (Figure 6f). When the secondary particles begin to crack due to internal stress, the primary particles are going to be exposed to the blank electrolyte, which will consume more electrolyte, form a thicker CEI layer, and cause more side reactions, leading to an increase in interface impedance and a gradual collapse of the structure. But the TMB additive is beneficial to inhibit the decomposition of electrolyte and reduce internal stress, thereby enhancing the structural stability and interface stability of the cathode material. This also explains why the cathode material with 10% TMB-containing electrolyte can maintain structural stability even after long cycling.

In order to directly observe the difference of CEI films, TEM images of the cathode materials are measured in Figure 7. For the pristine electrode, there is a legible boundary on the surface of the nickel-rich cathode material. After the first cycle, the surface of the particles with and without TMB additive is covered with an amorphous film, which is defined as CEI film, as shown in Figure S5 (Supporting Information). It can be

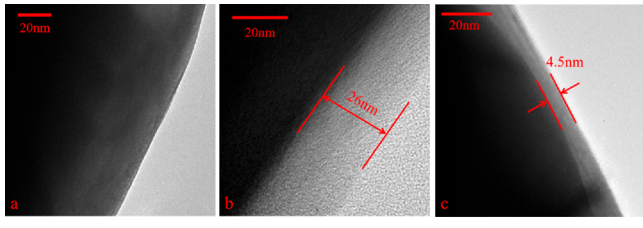

Figure 7. TEM images of pristine NCA (a), the cathode material after 300 cycles in blank electrolyte (b) and 10% TMB-containing electrolyte (c).

observed that the thickness of CEI films in the both blank electrolyte and TMB-containing electrolyte is about 2 nm. And the surface films are unstable and uneven. This can be attributed to the complicated formation process of CEI film in the activation stage of electrodes. On the contrary, after 300 cycles, the CEI film derived from the 10% TMB-containing electrolyte shows a layer with a thickness around 4–6 nm, which is thinner and more compact than that in the blank electrolyte with a thickness about 26 nm. And the thick CEI film is usually generated by the decomposition and consumption of electrolyte, thus leaving an negative effect on the diffusion rate of Li ion.[48,49] It means that the TMB additive can suppress the continued decomposition of the electrolyte, thus leading to form a more stable CEI film. This can also explain why the electrode with TMB-containing electrolyte maintains a relatively lower resistance over cycling.

To further investigate the effect of TMB on the CEI formation, XPS is conducted to verify the surface composition of the fresh and cycled electrodes after the initial cycle and 300 cycles, as shown in Figure 8 and Table S4. In the C 1s spectra, the signals located at 284.8, 285.6, 286.8, 289.1, 290.8, and 291.3 eV are assigned to C-C, C-H, C-O, C═O, CF_2, and CF_3, respectively. C−C bonds are mainly from the conductive agent Super P added during preparation of electrode plates. To compare the bonding percentage (bonding signal divided by overall concentration) of C═O and C-O in the different cases, it is clear that the bonds are mainly derived from the CEI films formed during cycling including $ROCO_2Li$, ROLi, and Li_2CO_3.[50−52] Therein, after 300 cycles, bonding percentages of both C-O and C═O for the TMB-blank case are obviously lower than those for the TMB-containing electrolyte. The results indicate that addition of TMB into the electrolyte could influence formation of CEI film in composition and thickness. In Figure 8b, the signals of O 1s spectra can be assigned to M-O (metal oxide), C═O, O-H, and C-O, corresponding to the binding energy of 529.4, 531.3, 531.8, and 533.6 eV, respectively.[53−56] The ratio of C-O and C═O at O 1s is generally correlated with C-O and C═O signals at C 1s.

https://dx.doi.org/10.1021/acssuschemeng.0c09241
ACS Sustainable Chem. Eng. 2021, 9, 1958−1968

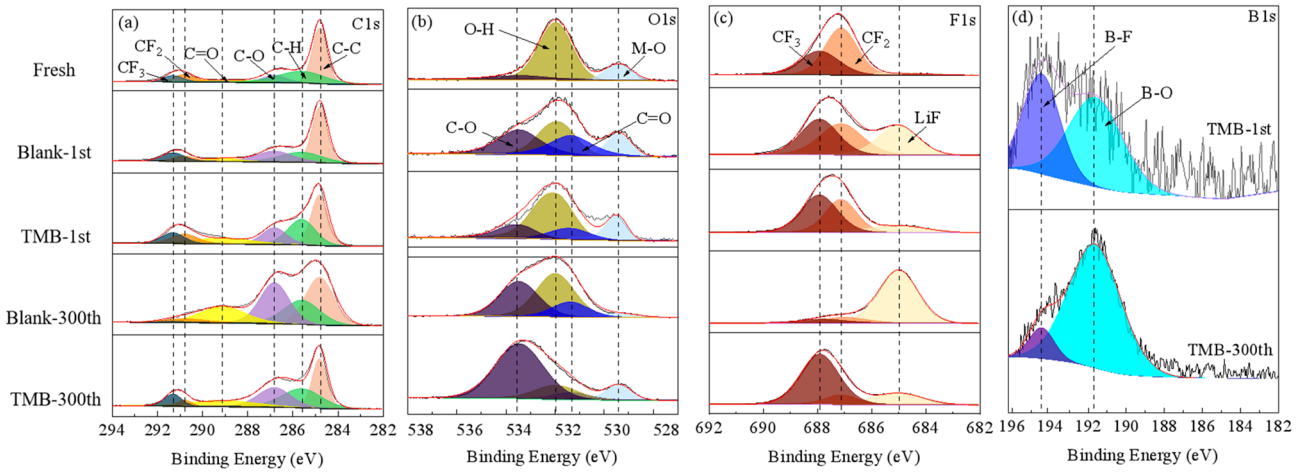

Figure 8. C 1s (a), O 1s (b), F 1s (c), and B 1s (d) XPS spectra of the fresh electrode and the electrodes after the initial cycle and 300 cycles in TMB-blank and 10% TMB-containing electrolytes.

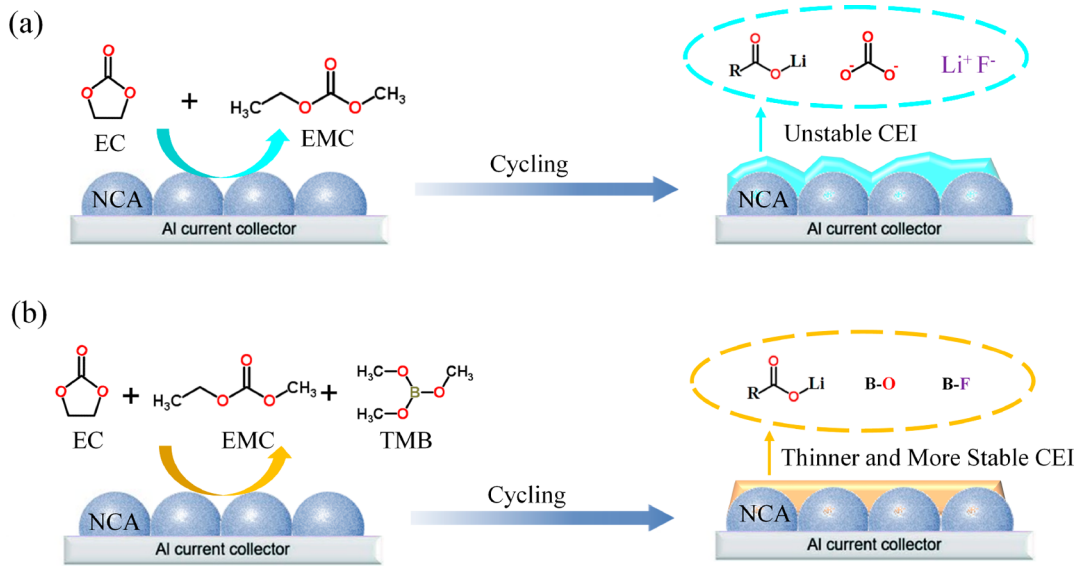

Figure 9. Scheme of blank electrolyte (a) and TMB additives (b) on the interfacial stability of cathodes.

Binding energy of M−O bonds in the O 1s spectra in all the cases is 529.4 eV. To compare bonding percentage of M-O, it can be found that the values after the initial cycle for both Blank and TMB are very close to that for the fresh electrode, but after 300 cycles, the bonding percentage of M-O is relatively reduced due to the formation of CEI films during long cycling. Importantly, the bonding percentage of M-O for Blank is 4.6%, much lower than 10.1% for TMB, indicating a thinner CEM film for the latter.[57,58] This is consistent with the results shown by TEM in Figure 7. The O-H signals are from inevitable surface pollution because the preparation of the materials and the specimens for XPS measurements is conducted in air, and PVDF in the tested electrode plates before or after cycling is also of moisture absorption. In the F 1s spectra, the bonding percentage of Li-F at 685.0 eV for the case after 300 cycles with 10% TMB-containing electrolyte is much lower than that with TMB-blank electrolyte, demonstrating composition change of the CEI film made by TMB. The other signals in the F 1s spectra are from PVDF in the electrodes.[44] For the B 1s spectra, the peaks at 191.6 and 194.2 eV are assigned to B−O and B−F bonds, respectively. Certainly, TMB participates in the generation of the CEI films involving B−O and B−F bonds.[59,60] However, the B-O and B-F signals are so weak compared to the other oxygen- or fluorine-involved bonds that B-O and B-F cannot be clearly assigned in the O 1s and F 1s spectra. From the initial cycle to 300 cycles, bonding percentage of B-F is much reduced and B-O is dominant after the long cycling. As pointed out in the previous work, TMB can coordinate with F^- ions to form a B−F bond and dissolve LiF at the initial cycle, and the proportion of F in CEI film decreases with cyling.[40] Generally, it is clear that adding TMB in the electrolyte can change the composition and thickness of CEI film to achieve a more stable and conductive one in the interface, which is consistent with the EIS and TEM results. The XPS survey spectra and the atomic concentration of each element for three samples are shown in Figure S6 and Table S3 (Supporting Information), respectively. Fourier transform infrared spectroscopy (FTIR) also confirms the above conclusion, as shown in Figure S7 (Supporting Information). It is obvious that several bands at around 843, 1041, 1266, 1415, 1619, and 1728 cm^{-1} appear on the FTIR patterns of the cathode material in the blank

https://dx.doi.org/10.1021/acssuschemeng.0c09241
ACS Sustainable Chem. Eng. 2021, 9, 1958−1968

electrolyte, which are assigned to $ROCO_2Li$ and Li_2CO_3 groups. However, they are significantly weakened on the FTIR patterns of the fresh electrode and electrode in the 10% TMB-containing electrolyte. In a word, TMB additives help to inhibit the decomposition of the electrolyte, thereby forming a thin and stable CEI film at the interface.

A possible reaction mechanism for TMB decomposition is proposed. The calculated oxidation potential of TMB is at 6.3 V, which is lower than that of EC (7.1 V) and EMC (6.8 V).[61] This suggests that the TMB is easily oxidized than solvent to form a stable CEI film. Then the TMB loses an electron, producing $C_2H_6BO_2^+$ ion. And the $C_2H_6BO_2^+$ ion can coordinate with F^- to form $C_2H_6BO_2F$. Eventually, $C_2H_6BO_2F$ decomposes and coordinates with the −OH on the surface of oxides to generate B-O and B-F groups. The schematic diagram is shown in Figure S8 (Supporting Information) and Figure 9.[61,62] In a word, the TMB can be decomposed to participate in the formation of the stable and protective CEI film over cycling. In addition, the SEM images show that, after long cycling, the secondary particles that make up the cathode material are cracked or even pulverized due to the increase of internal stress. This will further accelerate the instability of the layered structure and have a harmful influence on the cycle and rate performance. On the contrary, under the role of TMB electrolyte additive, the oxidative decomposition of the electrolyte can be significantly inhibited, thereby suppressing the occurrence of side reactions. According to the EIS spectra and TEM images, it is found that a thinner and more conductive CEI layer forms on the surface of cathode materials with TMB additives. In this situation, TMB can coordinate with F^- and reduce the content of the resistive LiF component on the cathode surface. It is beneficial to form a more stable CEI film, thereby enhancing the overall structure and interface stability. In addition, the stable and solid CEI film can avoid some potential side reactions between Ni-rich cathode materials and TMB, which makes the addition of the flammable TMB should not bring new safety risk.

CONCLUSION

In this article, TMB is used as an electrolyte additive to improve the electrochemical performance of the $LiNi_{0.88}Co_{0.09}Al_{0.03}O_2$ cathode material. Through systematic analysis, the interfacial and structural stability of the cathode material with TMB has been greatly improved. This result can be ascribed to two aspects: (1) TMB is involved in the formation of CEI film, forming a protective layer on the surface to protect secondary particles from crystal destruction and prevent the electrolyte from decomposition; (2) TMB can coordinate with F^- ions to dissolve LiF out of the CEI film and promote the formation of a thin CEI film and thus improves the rate capability of $LiNi_{0.88}Co_{0.09}Al_{0.03}O_2$. As a result, a capacity retention of up to 82% is achieved in $LiNi_{0.88}Co_{0.09}Al_{0.03}O_2$ cathode materials with 10% TMB after 300 cycles at 1C rate. This simple and efficient strategy is of great significance for improving the interfacial stability of nickel-rich cathode materials and promotes its further commercialization process.

EXPERIMENTAL SECTION

Preparation of Electrolytes. The blank electrolyte was 1 M $LiPF_6$ in ethylene carbonate (EC) and ethyl methyl carbonate (EMC) (volume ratio of 3:7, obtained from TianJin JinNiu Power Sources Material CO., Ltd., China). TMB was purchased from Alfa Aesar Chemicals CO., Ltd., China (>99.9995%). All these chemicals were used without further purification. Various contents of TMB were added into the blank electrolyte in volume percentage to obtain 2%, 5%, 10%, and 15% TMB-containing electrolytes. Electrolytes preparations were conducted in an argon-filled glovebox, in which water and oxygen contents were controlled to be less than 0.1 ppm.

Preparation of Electrodes. The electrodes were prepared by mixing 80 wt % $LiNi_{0.88}Co_{0.09}Al_{0.03}O_2$ (TianJin B&M Science and Technology Joint-Stock CO., LTO., China), 10 wt % Super P, and 10 wt % polyvinylidene fluoride (PVDF) in *N*-methylpyrrolidone (NMP), coating the slurry on Al foil, and vacuum drying at 110 °C for 12 h. Metallic lithium was used as anode. $LiNi_{0.88}Co_{0.09}Al_{0.03}O_2$/Li 2032 type coin cells were assembled with Celgard 2400 as separator in the argon-filled glovebox.

Electrochemical Measurements. The electrochemical performance of $LiNi_{0.88}Co_{0.09}Al_{0.03}O_2$/Li coin cells was evaluated on a LAND test system (CT2001A, China) at room temperature in the voltage range of 3.0−4.3 V. And the charge cutoff voltages were raised to 4.4, 4.5, 4.6, and 4.7 V to evaluate the high-voltage cycle performance. Electrochemical impedance measurements were performed on the IM6ex electrochemical station (Autolab, Germany) in a frequency range of 10^{-2}−10^5 Hz with a potential amplitude of 5 mV. The fitting data of the equivalent circuits for the impedance spectra were calculated by computer simulation using Zview electrochemical impedance software. Cyclic voltammograms (CV) were carried out on an LK2005A electrochemical workstation (Tianjin) at a scan rate of 0.5 mV s^{-1}.

Material Characterization. The viscosity (η) of the electrolytes was measured on a Brookfield DV2T at 30 °C. The ionic conductivity of electrolytes was measured using a DDS-11A (YOKE INSTRUMENT) with a Pt electrode at 30 °C. The wettability of electrolytes was measured with a JC2000D3M contact angle measuring instrument. Morphology and structure tests were performed on FE-SEM (JSM-7800F) at 15.0 kV and TEM (JEM-2800F). The X-ray photoelectron spectroscopy (XPS) measurements were performed on a Thermo Scientific ESCALAB 250Xi. The cycled electrodes were disassembled in the glovebox and washed three times with DMC solvent to remove the residual electrolyte, and then dried in vacuum at room temperature for 12 h.

ASSOCIATED CONTENT

Supporting Information

The Supporting Information is available free of charge at https://pubs.acs.org/doi/10.1021/acssuschemeng.0c09241.

The density, viscosity, and conductivity results; contact angle test; cycle performance in different voltage ranges; d*Q*/d*V* profiles; the fitting data and Bode plots of EIS spectra; TEM of electrodes after the first cycle; the XPS survey spectra; atomic concentration of each element of fresh electrode and electrodes after 300 cycles in blank and 10% TMB-containing electrolytes; XPS spectra of electrodes after the first cycle; FTIR results for fresh electrode and electrodes after 300 cycles in blank and 10% TMB-containing electrolytes; and mechanisms for electrochemical oxidative decomposition of TMB (PDF)

AUTHOR INFORMATION

Corresponding Author

Guo-Ran Li − *Institute of New Energy Material Chemistry, School of Materials Science and Engineering, Renewable Energy Conversion and Storage Center, Nankai University, Tianjin 300350, China;* orcid.org/0000-0002-6380-5725; Email: guoranli@nankai.edu.cn; Fax: +86-22-23500780

https://dx.doi.org/10.1021/acssuschemeng.0c09241
ACS Sustainable Chem. Eng. 2021, 9, 1958−1968

Authors

Zhen-Xue Xiao − *Institute of New Energy Material Chemistry, School of Materials Science and Engineering, Renewable Energy Conversion and Storage Center, Nankai University, Tianjin 300350, China*

Shao-Lun Cui − *Institute of New Energy Material Chemistry, School of Materials Science and Engineering, Renewable Energy Conversion and Storage Center, Nankai University, Tianjin 300350, China*

Yang-Yang Wang − *Institute of New Energy Material Chemistry, School of Materials Science and Engineering, Renewable Energy Conversion and Storage Center, Nankai University, Tianjin 300350, China*

Sheng Liu − *Institute of New Energy Material Chemistry, School of Materials Science and Engineering, Renewable Energy Conversion and Storage Center, Nankai University, Tianjin 300350, China;* orcid.org/0000-0001-5933-1101

Xue-Ping Gao − *Institute of New Energy Material Chemistry, School of Materials Science and Engineering, Renewable Energy Conversion and Storage Center, Nankai University, Tianjin 300350, China;* orcid.org/0000-0001-7305-7567

Complete contact information is available at: https://pubs.acs.org/10.1021/acssuschemeng.0c09241

Author Contributions

†Z.-X.X. and S.-L.C. contributed equally to this work.

Notes

The authors declare no competing financial interest.

■ ACKNOWLEDGMENTS

Financial support from the New Energy Project for Electric Vehicles in the National Key Research and Development Program (2016YFB0100200) and the NSFC (21573114, 51502145, and 21421001) of China is gratefully acknowledged.

■ REFERENCES

(1) Cui, S. L.; Wang, Y. Y.; Liu, S.; Li, G. R.; Gao, X. P. Evolution Mechanism of Phase Transformation of Li-Rich Cathode Materials in Cycling. *Electrochim. Acta* **2019**, *328*, 135109−135118.

(2) Cui, S. L.; Zhang, X.; Wu, X. W.; Liu, S.; Zhou, Z.; Li, G. R.; Gao, X. P. Understanding the Structure-Performance Relationship of Lithium-Rich Cathode Materials from an Oxygen-Vacancy Perspective. *ACS Appl. Mater. Interfaces* **2020**, *12*, 47655−47666.

(3) Lee, Y. S.; Ahn, D.; Cho, Y. H.; Hong, T. E.; Cho, J. Improved Rate Capability and Thermal Stability of $LiNi_{0.5}Co_{0.2}Mn_{0.3}O_2$ Cathode Materials via Nanoscale SiP_2O_7 Coating. *J. Electrochem. Soc.* **2011**, *158*, A1354−A1360.

(4) Myung, S. T.; Izumi, K.; Komaba, S.; Sun, Y. K.; Yashiro, H.; Kumagai, N. Role of Alumina Coating on Li-Ni-Co-Mn-O Particles as Positive Electrode Material for Lithium-Ion Batteries. *Chem. Mater.* **2005**, *17*, 3695−3704.

(5) Oh, Y.; Ahn, D.; Nam, S.; Park, B. The Effect of Al_2O_3-coating Coverage on the Electrochemical Properties in $LiCoO_2$ Thin Films. *J. Solid State Electrochem.* **2010**, *14*, 1235−1240.

(6) Zhecheva, E.; Stoyanova, R.; Tyuliev, G.; Tenchev, K.; Mladenov, M.; Vassilev, S. Surface Interaction of $LiNi_{0.8}Co_{0.2}O_2$ Cathodes with MgO. *Solid State Sci.* **2003**, *5*, 711−720.

(7) Yoon, W. S.; Nam, K. W.; Jang, D.; Chung, K. Y.; Hanson, J.; Chen, J. M.; Yang, X. Q. Structural Study of the Coating Effect on the Thermal Stability of Charged MgO-coated $LiNi_{0.8}Co_{0.2}O_2$ Cathodes Investigated by In Situ XRD. *J. Power Sources* **2012**, *217*, 128−134.

(8) Wen, W. C.; Yang, X. K.; Wang, X. Y.; Shu, L. G. H. Improved Electrochemical Performance of the Spherical $LiNi_{0.5}Mn_{1.5}O_4$ Particles Modified by Nano-Y_2O_3 Coating. *J. Solid State Electrochem.* **2015**, *19* (4), 1235−1246.

(9) Yao, Y. L.; Liu, H. C.; Li, G. C.; Peng, H. R.; Chen, K. Z. Synthesis and Electrochemical Performance of Phosphate-coated Porous $LiNi_{1/3}Co_{1/3}Mn_{1/3}O_2$ Cathode Material for Lithium Ion Batteries. *Electrochim. Acta* **2013**, *113*, 340−345.

(10) Zeng, Y. W.; He, J. H. Surface Structure Investigation of $LiNi_{0.8}Co_{0.2}O_2$ by $AlPO_4$ Coating and Using Functional Electrolyte. *J. Power Sources* **2009**, *189*, 519−521.

(11) Tan, K. S.; Reddy, M. V.; Rao, G. V. S.; Chowdari, B. V. R. Effect of $AlPO_4$-coating on Cathodic Behaviour of $Li(Ni_{0.8}Co_{0.2})O_2$. *J. Power Sources* **2005**, *141*, 129−142.

(12) Kim, H. S.; Kim, W. S.; Gu, H. B.; Wang, G. Electrochemical Performance of $SnPO_4$-coated $LiNi_{1/3}Mn_{1/3}Co_{1/3}O_2$ Cathode Materials. *J. New Mater. Electrochem. Syst.* **2009**, *12*, 207−212.

(13) Lee, D. J.; Scrosati, B.; Sun, Y. K. $Ni_3(PO_4)_2$-coated $Li[Ni_{0.8}Co_{0.15}Al_{0.05}]O_2$ Lithium Battery Electrode with Improved Cycling Performance at 55 °C. *J. Power Sources* **2011**, *196*, 7742−7746.

(14) Kim, Y.; Cho, J. Lithium-reactive $Co_3(PO_4)_2$ Nanoparticle Coating on High-capacity $LiNi_{0.8}Co_{0.16}Al_{0.04}O_2$ Cathode Material for Lithium Rechargeable Batteries. *J. Electrochem. Soc.* **2007**, *154*, A495−A499.

(15) Liu, X.; Li, H.; Yoo, E.; Ishida, M.; Zhou, H. Fabrication of $FePO_4$ Layer Coated $LiNi_{1/3}Co_{1/3}Mn_{1/3}O_2$: towards High-performance Cathode Materials for Lithium ion Batteries. *Electrochim. Acta* **2012**, *83*, 253−258.

(16) Shi, S. J.; Tu, J. P.; Mai, Y. J.; Zhang, Y. Q.; Tang, Y. Y.; Wang, X. L. Structure and Electrochemical Performance of CaF_2 Coated $LiMn_{1/3}Ni_{1/3}Co_{1/3}O_2$ Cathode Material for Li-ion Batteries. *Electrochim. Acta* **2012**, *83*, 105−112.

(17) Aboulaich, A.; Ouzaouit, K.; Faqir, H.; Kaddami, A.; Benzakour, I.; Akalay, I. Improving Thermal and Electrochemical Performances of $LiCoO_2$ Cathode at High Cut-off Charge Potentials by MF_3 (M = Ce, Al) Coating. *Mater. Res. Bull.* **2016**, *73*, 362−368.

(18) Choi, W.; Benayard, A.; Park, J. H.; Park, J.; Doo, S. G.; Mun, J. Versatile Coating of Lithium Conductive Li_2TiF_6 on Over-lithiated Layered Oxide in Lithium-Ion Batteries. *Electrochim. Acta* **2014**, *117*, 492−497.

(19) Chung, Y.; Ryu, S. H.; Ju, J. H.; Bak, Y. R.; Hwang, M. J.; Kim, K. W.; Cho, K.; Ryu, K. K. S. A Surfactant-based Method for Carbon Coating of $LiNi_{0.8}Co_{0.15}Al_{0.05}O_2$ Cathode in Li Ion Batteries. *Bull. Korean Chem. Soc.* **2010**, *31*, 2304−2308.

(20) Ju, J. H.; Chung, Y. M.; Bak, Y. R.; Hwang, M. J.; Ryu, K. S. The Effects Of Carbon Nano-Coating on $Li(Ni_{0.8}Co_{0.15}Al_{0.05})O_2$ Cathode Material Using Organic Carbon for Li-Ion Battery. *Surf. Rev. Lett.* **2010**, *17*, 51−58.

(21) Yang, C.; Zhang, X.; Huang, M.; Huang, J.; Fang, Z. Preparation and Rate Capability of Carbon Coated $LiNi_{1/3}Co_{1/3}Mn_{1/3}O_2$ as Cathode Material in Lithium Ion Batteries. *ACS Appl. Mater. Interfaces* **2017**, *9*, 12408−12415.

(22) Liu, X.; Li, H.; Li, D.; Ishida, M.; Zhou, H. PEDOT Modified $LiNi_{1/3}Co_{1/3}Mn_{1/3}O_2$ with Enhanced Electrochemical Performance for Lithium Ion Batteries. *J. Power Sources* **2013**, *243*, 374−380.

(23) Xiong, X. H.; Ding, D.; Wang, Z. X.; Huang, B.; Guo, H. J.; Li, X. H. Surface Modification of $LiNi_{0.8}Co_{0.1}Mn_{0.1}O_2$ with Conducting Polypyrrole. *J. Solid State Electrochem.* **2014**, *18*, 2619−2624.

(24) Zhu, L.; Yan, T.-F.; Jia, D.; Wang, Y.; Wu, Q.; Gu, H.-T.; Wu, Y.-M.; Tang, W.-P. $LiFePO_4$-coated $LiNi_{0.5}Co_{0.2}Mn_{0.3}O_2$ Cathode Materials with Improved High Voltage Electrochemical Performance and Enhanced Safety for Lithium Ion Pouch Cells. *J. Electrochem. Soc.* **2019**, *166*, A5437−A5444.

(25) Duan, J.; Wu, C.; Cao, Y.; Du, K.; Peng, Z.; Hu, G. Enhanced Electrochemical Performance and Thermal Stability of $LiNi_{0.80}Co_{0.15}Al_{0.05}O_2$ via Nano-sized $LiMnPO_4$ Coating. *Electrochim. Acta* **2016**, *221*, 14−22.

(26) Liang, L.; Sun, X.; Wu, C.; Hou, L.; Sun, J.; Zhang, X.; Yuan, C. Nasicon-type Surface Functional Modification in Core-Shell Li-$Ni_{0.5}Mn_{0.3}Co_{0.2}O_2$@$NaTi_2(PO_4)_3$ Cathode Enhances Its High-voltage Cycling Stability and Rate Capacity toward Li-ion Batteries. *ACS Appl. Mater. Interfaces* **2018**, *10*, 5498−5510.
(27) Wang, M.; Gong, Y.; Gu, Y.; Chen, Y.; Chen, L.; Shi, H. Effects of Fast Lithium-ion Conductive Coating Layer on the Nickel Rich Layered Oxide Cathode Material. *Ceram. Int.* **2019**, *45*, 3177−3185.
(28) Yuan, H.; Song, W.; Wang, M.; Gu, Y.; Chen, Y. Lithium-ion Conductive Coating Layer on Nickel Rich Layered Oxide Cathode Material with Improved Electrochemical Properties for Li-ion Battery. *J. Alloys Compd.* **2019**, *784*, 1311−1322.
(29) Jamil, S.; Ran, Q. W.; Yang, Li; Huang, Y.; Cao, S.; Yang, X. K.; Wang, X. Y. Improved High-voltage Performance of Li-$Ni_{0.87}Co_{0.1}Al_{0.03}O_2$ by Li^+-conductor Coating. *Chem. Eng. J.* **2021**, *407*, 126442−126452.
(30) Huang, Y.; Zhang, X. H.; Yu, R. Z.; Jamil, S.; Cao, S.; Fang, S. S.; Wang, Y.; Tang, K.; Chen, G. R.; Luo, Z. G.; Yang, X. K.; Wang, X. Y. Preparation and Performance of the Heterostructured Material with a Ni-Rich Layered Oxide Core and a $LiNi_{0.5}Mn_{1.5}O_4$-like Spinel Shell. *ACS Appl. Mater. Interfaces* **2019**, *11*, 16556−16566.
(31) Han, Z.; Yu, J.; Zhan, H.; Liu, X.; Zhou, Y. Sb_2O_3-modified $LiNi_{1/3}Co_{1/3}Mn_{1/3}O_2$ Material with Enhanced Ehermal Safety and Electrochemical Property. *J. Power Sources* **2014**, *254*, 106−111.
(32) Yun, S. H.; Park, K. S.; Park, Y. J. The Electrochemical Property of ZrF_x-coated $Li[Ni_{1/3}Co_{1/3}Mn_{1/3}]O_2$ Cathode Material. *J. Power Sources* **2010**, *195*, 6108−6115.
(33) Wu, F.; Wang, M.; Su, Y. F.; Chen, S.; Xu, B. Effect of TiO_2-coating on the Electrochemical Performances of Li-$Co_{1/3}Ni_{1/3}Mn_{1/3}O_2$. *J. Power Sources* **2009**, *191*, 628−632.
(34) Zhang, S. S. A Review on Electrolyte Additives for Lithium-ion Batteries. *J. Power Sources* **2006**, *162*, 1379−1394.
(35) Mai, S.; Xu, M.; Liao, X.; Hu, J.; Lin, H.; Xing, L.; Liao, Y.; Li, X.; Li, W. Tris(trimethylsilyl) Phosphite as Electrolyte Additive for High Voltage Layered Lithium Nickel Cobalt Manganese Oxide Cathode of Lithium Ion Battery. *Electrochim. Acta* **2014**, *147*, 565−571.
(36) Huang, W.; Xing, L.; Wang, Y.; Xu, M.; Li, W.; Xie, F.; Xia, S. 4-(Trifluoromethyl)-benzonitrile: A Novel Electrolyte Additive for Lithium Nickel Manganese Oxide Cathode of High Voltage Lithium Ion Battery. *J. Power Sources* **2014**, *267*, 560−565.
(37) Liao, X.; Huang, Q.; Mai, S.; Wang, X.; Xu, M.; Xing, L.; Liao, Y.; Li, W. Understanding Self-discharge Mechanism of Layered Nickel Cobalt Manganese Oxide at High Potential. *J. Power Sources* **2015**, *286*, 551−556.
(38) Rong, H.; Xu, M.; Xie, B.; Huang, W.; Liao, X.; Xing, L.; Li, W. Performance Improvement of Graphite/$LiNi_{0.4}Co_{0.2}Mn_{0.4}O_2$ Battery at High Voltage with Added Tris(trimethylsilyl) phosphate. *J. Power Sources* **2015**, *274*, 1155−1161.
(39) Liu, Q. Y.; Yang, G. J.; Liu, S.; Han, M.; Wang, Z. X.; Chen, L. Q. Trimethyl Borate as Film-Forming Electrolyte Additive To Improve High-Voltage Performances. *ACS Appl. Mater. Interfaces* **2019**, *11*, 17435−17443.
(40) Chang, C.-C.; Lee, K.-Y.; Lee, H.-Y.; Su, Y.-H.; Her, L.-J. Trimethyl Borate and Triphenyl Borate as Electrolyte Additives for $LiFePO_4$ Cathode with Enhanced High Temperature Performance. *J. Power Sources* **2012**, *217*, 524−529.
(41) Wang, Z.; Xing, L.; Li, J.; Li, B.; Xu, M.; Liao, Y.; Li, W. Trimethyl Borate as An Electrolyte Additive for High Potential Layered Cathode with Concurrent Improvement of Rate Capability and Cyclic Stability. *Electrochim. Acta* **2015**, *184*, 40−46.
(42) Mai, S.; Xu, M.; Liao, X.; Xing, L.; Li, W. Improving Cyclic Stability of Lithium Nickel Manganese Oxide Cathode at Elevated Temperature by Using Dimethyl Phenylphosphonite as Electrolyte Additive. *J. Power Sources* **2015**, *273*, 816−822.
(43) Li, B.; Wang, Y.; Tu, W.; Wang, Z.; Xu, M.; Xing, L.; Li, W. Improving Cyclic Stability of Lithium Nickel Manganese Oxide Cathode for High Voltage Lithium Ion Battery by Modifying Electrode/electrolyte Interface with Electrolyte Additive. *Electrochim. Acta* **2014**, *147*, 636−642.
(44) Zhao, W.; Zheng, J.; Zou, L.; Jia, H.; Liu, B.; Wang, H.; Engelhard, M. H.; Wang, C.; Xu, W.; Yang, Y.; Zhang, J.-G. High Voltage Operation of Ni-Rich NMC Cathodes Enabled by Stable Electrode/Electrolyte Interphases. *Adv. Energy Mater.* **2018**, *8*, 1800297−1800305.
(45) Arai, H.; Muller, S.; Haas, O. AC Impedance Analysis of Bifunctional Air Electrodes for Metal-Air Batteries. *J. Electrochem. Soc.* **2000**, *147*, 3584−3591.
(46) Liu, S.; Su, J.; Zhao, J.; Chen, X.; Zhang, C.; Huang, T.; Wu, J.; Yu, A. Unraveling the Capacity Fading Mechanisms of Li-$Ni_{0.6}Co_{0.2}Mn_{0.2}O_2$ at Elevated Temperatures. *J. Power Sources* **2018**, *393*, 92−98.
(47) Cai, Z.; Liu, Y.; Zhao, J.; Li, L.; Zhang, Y.; Zhang, J. Tris(trimethylsilyl) Borate as Electrolyte additive to Improve Performance of Lithium-ion Batteries. *J. Power Sources* **2012**, *202*, 341−346.
(48) Zuo, X. X.; Fan, C. J.; Liu, J. S.; Xiao, X.; Wu, J. H.; Nan, J. M. Effect of tris(trimethylsilyl)borate on the high voltage capacity retention of $LiNi_{0.5}Co_{0.2}Mn_{0.3}O_2$/graphite cells. *J. Power Sources* **2013**, *229*, 308−312.
(49) Li, J. H.; Xing, L. D.; Zhang, R. Q.; Chen, M.; Wang, Z. S.; Xu, M. Q.; Li, W. S. Tris(trimethylsilyl)borate as an electrolyte additive for improving interfacial stability of high voltage layered lithium-rich oxide cathode/carbonate-based electrolyte. *J. Power Sources* **2015**, *285*, 360−366.
(50) Martha, S. K.; Nanda, J.; Veith, G. M.; Dudney, N. J. Surface Studies of High Voltage Lithium Rich Composition: $Li_{1.2}Mn_{0.525}Ni_{0.175}Co_{0.1}O_2$. *J. Power Sources* **2012**, *216*, 179−186.
(51) Xu, M.; Hao, L.; Liu, Y.; Li, W.; Xing, L.; Li, B. Experimental and Theoretical Investigations of Dimethylacetamide (DMAc) as Electrolyte Stabilizing Additive for Lithium Ion Batteries. *J. Phys. Chem. C* **2011**, *115*, 6085−6094.
(52) Yang, L.; Markmaitree, T.; Lucht, B. L. Inorganic Additives for Passivation of High Voltage Cathode Materials. *J. Power Sources* **2011**, *196*, 2251−2254.
(53) Jiao, S. H.; Ren, X. D.; Cao, R. G.; Engelhard, M. H.; Liu, Y. Z.; Hu, D. H.; Mei, D. H.; Zheng, J. M.; Zhao, W. G.; Li, Q. Y.; Liu, N.; Adams, B. D.; Ma, C.; Liu, J.; Zhang, J. G.; Xu, W. Stable Cycling of High-voltage Lithium Metal Batteries in Ether Electrolytes. *Nature Energy.* **2018**, *3*, 739−746.
(54) Li, W.; Xiao, A.; Lucht, B. L.; Smart, M. C.; Ratnakumar, B. V. Surface Analysis of Electrodes from Cells Containing Electrolytes with Stabilizing Additives Exposed to High Temperature. *J. Electrochem. Soc.* **2008**, *155*, A648−A657.
(55) Xu, M.; Zhou, L.; Dong, Y.; Chen, Y.; Garsuch, A.; Lucht, B. L. Improving the Performance of Graphite/$LiNi_{0.5}Mn_{1.5}O_4$ Cells at High Voltage and Elevated Temperature with Added Lithium Bis(oxalato) Borate (LiBOB). *J. Electrochem. Soc.* **2013**, *160*, A2005−A2013.
(56) Xu, M.; Zhou, L.; Dong, Y.; Chen, Y.; Demeaux, J.; MacIntosh, A. D.; Garsuch, A.; Lucht, B. L. Development of Novel Lithium Borate Additives for Designed Surface Modification of High Voltage $LiNi_{0.5}Mn_{1.5}O_4$ Cathodes. *Energy Environ. Sci.* **2016**, *9*, 1308−1319.
(57) Han, J.-G.; Lee, S. J.; Lee, J.; Kim, J.-S.; Lee, K. T.; Choi, N.-S. Tunable and Robust Phosphite-Derived Surface Film to Protect Lithium-Rich Cathodes in Lithium-Ion Batteries. *ACS Appl. Mater. Interfaces* **2015**, *7*, 8319−8329.
(58) Yang, X. R.; Li, J. H.; Xing, L. D.; Liao, Y.; Xu, M. Q.; Huang, Q. M.; Li, W. S. Stabilizing Lithium Manganese Oxide/Organic Carbonate Electrolyte Interface with A Simple Boron-containing Additive. *Electrochim. Acta* **2017**, *227*, 24−32.
(59) Li, J. H.; Xing, L. D.; Zhang, L. P.; Yu, Le; Fan, W. Z.; Xu, M. Q.; Li, W. S. Insight into Self-discharge of Layered Lithium-rich Oxide Cathode in Carbonate-based Electrolytes With and Without Additive. *J. Power Sources* **2016**, *324*, 17−25.
(60) Li, J. H.; Wang, Z. S. Triethyl Borate and Tripropyl Borate as Electrolyte Additives for 4.8 V High Voltage Layered Lithium-rich Oxide Cathode with Enhanced Self-discharge Suppression Perform-

https://dx.doi.org/10.1021/acssuschemeng.0c09241
ACS Sustainable Chem. Eng. 2021, 9, 1958−1968

ance: A Comparative Study. *J. Power Sources* **2020**, *450*, 227648−227657.
(61) Li, J. H.; Liao, Y. Q.; Fan, W. Z.; Li, Z. F.; Li, G. J.; Zhang, Q. K.; Xing, L. D.; Xu, M. Q.; Li, W. S. Significance of Electrolyte Additive Molecule Structure in Constructing Robust Interphases on High-Voltage Cathodes. *ACS Appl. Energy Mater.* **2020**, *3*, 3049−3058.
(62) Liu, Q. Y.; Yang, G. J.; Liu, S.; Han, M.; Wang, Z. X.; Chen, L. Q. Trimethyl Borate as Film-Forming Electrolyte Additive to Improve High-Voltage Performances. *ACS Appl. Mater. Interfaces* **2019**, *11*, 17435−17443.

https://dx.doi.org/10.1021/acssuschemeng.0c09241
ACS Sustainable Chem. Eng. 2021, 9, 1958−1968